Euro. Jnl of Applied Mathematics (2016), *vol.* 27, *pp.* 111–130. © Cambridge University Press 2015
doi:10.1017/S0956792515000406

Inverse obstacle backscattering problems with phaseless data

JAEMIN SHIN

Department of Mathematical Sciences, Hanbat National University, Daejeon, Republic of Korea
email: *jaemin.shin@hanbat.ac.kr*

(*Received 23 June 2014; revised 2 July 2015; accepted 7 July 2015; first published online 31 July 2015*)

In this article, we provide a numerical algorithm to reconstruct a convex sound-soft scatterer from phaseless backscattering data, assuming sufficiently high frequency. Certain uniqueness and existence results for the case of circular scatterers are given as well, based on the asymptotic expansion for the normal derivative of the total field.

Key words: Inverse obstacle scattering, backscattering, phaseless far field pattern, high-frequency

1 Introduction

Consider the following exterior Helmholtz equation in $\mathbb{R}^2$,

$$\Delta u + k^2 u = 0 \text{ in } \mathbb{R}^2 \setminus \overline{\Omega}, \tag{1.1a}$$

$$u = 0 \text{ on } \partial\Omega, \tag{1.1b}$$

$$u = u^i + u^s, \quad u^i = e^{ikd\cdot x}, \tag{1.1c}$$

$$\lim_{r\to\infty} r^{1/2}\left(\frac{\partial u^s}{\partial r} - iku^s\right) = 0, \ r = |x|. \tag{1.1d}$$

Here, we assume that the scatterer Ω is strictly convex and the boundary, $\partial\Omega$ is smooth enough. By d, we denote the incident direction such that $|d| = 1$. The last condition (1.1d), the so-called Sommerfeld radiation condition is satisfied uniformly with respect to all directions $\hat{x} = x/r$, which gives the uniqueness for the exterior Helmholtz equation. Furthermore, this is equivalent to the existence of the far field pattern u_∞ defined by

$$u^s(x,d,k) = \frac{e^{ikr}}{r^{1/2}}\left\{u_\infty(\hat{x},d,k) + O\left(\frac{1}{r}\right)\right\}, \quad r\to\infty.$$

The inverse problem arising from (1.1) is to seek the scatterer Ω or $\partial\Omega$ from the far field pattern $u_\infty(\hat{x},d,k)$ in a certain set $E \subset S^1 \times S^1 \times \mathbb{R}^+$. This has many applications such as medical imaging, seismic imaging, and non-destructive testing.

This problem has been studied intensively for several decades analytically as well as numerically, under various assumptions and sets E (see e.g. [1] for a comprehensive survey). In particular, Colton and Sleeman [2] showed that the far field patterns for a

https://doi.org/10.1017/S0956792515000406 Published online by Cambridge University Press

finite number of incident plane waves can uniquely identify the scatterers with *a priori* information that unknown scatterers lie inside a given ball. However, the general case, i.e. the uniqueness for $E = S^1 \times \{d = d_0\} \times \{k = k_0\}$ for arbitrary d_0, k_0, is still open. In this case, we have the following equation:

$$F(\partial\Omega) = u_\infty(\widehat{x}, d_0, k_0), \quad \widehat{x} \in S^1. \tag{1.2}$$

Although there is no uniqueness for (1.2), one may think that (1.2) is an overdetermined problem with twice as many equations as unknowns, since $u_\infty(\widehat{x})$ is a complex-valued function but the unknown $\partial\Omega$ is a real-valued function. Furthermore, in many important applications, it is easy to measure the amplitude of the far field pattern instead of the full far field. In fact, as the frequency increases, it is more expensive to measure field phases in practical applications. Thus, we consider the amplitude of the far field pattern as data instead of the full far field.

This inverse problem with the amplitude of the far field as data was first introduced by Kress and Rundell in [9]. They used the Fréchet derivative with frozen regularised Newton and Landweber iterations in order to obtain approximate numerical solutions. They also showed that the modulus of the far field pattern is invariant under translation. Indeed, the far field pattern for the obstacle

$$\Omega_h := \{x + h : x \in \Omega\}$$

is given by

$$u_{\infty,h}(\widehat{x}, d, k) = e^{ikh\cdot(d-\widehat{x})} u_\infty(\widehat{x}, d, k), \tag{1.3}$$

where h is a fixed vector and u_∞ is the far field pattern for Ω. The relation (1.3) shows that it is not possible to recover the position from modulus data. After Kress and Rundell's work, Ivanyshyn and Kress solved the modulus data problem by a non-linear integral equation approach in [6]. Recently, Ivanyshyn and Kress successfully determined the position of a scatterer from the full far field data at a few measurement points. They were able to recover a scatterer by combining with a method for modulus data in [7]. However, there is no uniqueness results with the modulus data except the uniqueness for the forward-scattering problem, in which $|u_\infty(d, d, k_0)|$, $d \in S^1$ is given as data, assuming the scatterers are balls centred at the origin with radius R such that $k_0 R < 0.2303$ (see [11]), even with the translation invariance taken into account. This is due to breaking Rellich's lemma that the far field pattern uniquely determines the scattered field u^s, which is the main ingredient for the uniqueness of the full data problem, as pointed out in [9].

In this work, we consider a backscattering problem with the modulus of the far field pattern as data for a fixed k in 2-dimensional space. That is, we are interested in solving

$$|F_b(\partial\Omega; k)| = |u_\infty(-d, d, k)|, \quad d \in S^1 \tag{1.4}$$

for a smooth and strictly convex obstacle Ω and a fixed k. In this work, we have two objectives: for sufficiently large k,

(1) Development of numerical algorithm to reconstruct sound-soft scatterers from phaseless far field patterns as data.

(2) Identification of sound-soft circles from phaseless data.

https://doi.org/10.1017/S0956792515000406 Published online by Cambridge University Press

Similar to the case of the fixed incident field problem with modulus data, one cannot determine the location of the scatterer due to the invariance of translation, i.e.

$$|u_{\infty,h}(-d,d,k)| = |u_\infty(-d,d,k)|, \tag{1.5}$$

since

$$u_{\infty,h}(-d,d,k) = e^{2ikh\cdot d}u_\infty(-d,d,k).$$

Moreover, only a few results are known for the backscattering problem even if full far fields are given as data, unlike the standard scattering problem. Indeed, Kress and Rundell showed the Fréchet derivative of F_b at the unit circle is injective for sufficiently small k and reconstructed scatterers numerically in [10]. The injectivity of the derivative for general domains was given by Hähner and Kress by considering $F_b(\partial\Omega;k)$ over all $k \in (0,1)$. Apart from these results, there are no uniqueness results for the inverse obstacle backscattering problems to the author's knowledge. This is due to the lack of differential equations describing the backscattering problem directly. However, one can expect from Majda's result [12] that the geometric information of $\partial\Omega$ near $x_0 \in \partial\Omega$ is accumulated on $u_\infty(-d,d,k)$ for $d = -\nu(x_0)$ as long as the scatterer is strictly convex and the wave number is sufficiently high. Indeed, it is known [12] that

$$\left|u_\infty(\hat{x},d,k) + e^{ikx^+\cdot(d-\hat{x})}\kappa(x^+)^{-1/2}\frac{\hat{x}\cdot n}{|\hat{x}-d|^{1/2}}\right| \leqslant C\frac{1}{k}, \quad k \geqslant k_1.$$

Here, $n = (\hat{x}-d)/|\hat{x}-d|$, x^+ is the preimage of n under the Gauss map, and $\kappa(x^+)$ is the curvature of $\partial\Omega$ at x^+. For the backscattering case, i.e. $\hat{x} = -d$, it follows that

$$\left|u_\infty(-d,d,k) + e^{2ikx^+\cdot d}(2\kappa(x^+))^{-1/2}\right| \leqslant C\frac{1}{k}, \quad k \geqslant k_1. \tag{1.6}$$

The method used in this work is motivated by estimate (1.6). We introduce a map **F** from a frozen Newton scheme, using a specific parametric representation for convex scatterers. It turns out a fixed point of **F** is closely related to the solution of the inverse problem (1.4). As a consequence, we are numerically able to recover shapes of scatterers from $|u_\infty(-d,d,k)|$ through an iteration method based on **F** for sufficiently large k. In this algorithm, we do not need the Fréchet derivative of F_b or $|F_b|$. Furthermore, we show the uniqueness as well as existence for (1.4) if the scatterers are known to be circles *a priori*. More precisely, we have the following Theorem.

Theorem 1 *Let $p > 0$. Then there exists $k_0 > 0$ such that for any $k \geqslant k_0$*

$$|F_b(\partial B_R;k)| = p$$

is uniquely solvable in $\{B_R : R \geqslant p^2\}$, where B_R is a circle centred at zero with radius R.

It is obvious that the modulus of far field pattern for the backscattering is a constant if the scatterer is a circle, although the converse is not obvious. Thus, one may consider $|F_b(\partial B_R;k)|$ as a function of R with parameter k.

https://doi.org/10.1017/S0956792515000406 Published online by Cambridge University Press

Theorem 1 is a consequence of the numerical algorithm for general convex domains that is described in Section 4. Although we are not able to show the uniqueness for the inverse problems for general domains at this point, the numerical evidence indicates that our algorithm converges and thus one may have uniqueness for general convex domains at least if $k/\max\kappa \geqslant \tilde{k}_0$ for sufficiently large $\tilde{k}_0$. There are several uniqueness results for various inverse obstacle scattering problems, but many of them need the assumption that kR (where R is a diameter of the scatterer) is sufficiently small since their methods are related to the smallest eigenvalue of the Laplace operator. However, our algorithm and uniqueness result are valid for large k, which are more effective from a practical point of view, since phase information is difficult to measure or not available at all for a high frequency.

This article is organised as follows. In Section 2, we review the integral representations for F_b and its derivative and state the theory for the related high-frequency limit. We also give two important lemmas for the case of circular scatterers. In Section 3, we provide a proof of Theorem 1 by fixed point argument. We develop a numerical algorithm and give numerical examples in Section 4. Some concluding remarks are drawn in the last section.

2 Preliminaries

We begin with an integral representation for $u_\infty(\hat{x}, d, k)$ and $\frac{\partial u}{\partial \nu}$. Let

$$E(x, y) = \frac{i}{4} H_0^{(1)}(k|x - y|)$$

be the fundamental solution to the exterior Helmholtz equation, where we denote the Hankel function of the first kind of order 0 by $H_0^{(1)}$. By Green's formula

$$u^s(y, d, k) = \int_{\partial\Omega} u^s(y, d, k) \frac{\partial E(x, y)}{\partial \nu(y)} - \frac{\partial u^s(y, d, k)}{\partial \nu} E(x, y) ds(y), \quad x \in \mathbb{R}^2 \setminus \overline{\Omega},$$

$$0 = \int_{\partial\Omega} u^i(y, d, k) \frac{\partial E(x, y)}{\partial \nu(y)} - \frac{\partial u^i(y, d, k)}{\partial \nu} E(x, y) ds(y), \quad x \in \mathbb{R}^2 \setminus \overline{\Omega}.$$

Using the boundary condition (1.1c), the asymptotic behaviour of the fundamental solution gives

$$u^s(y, d, k) = -\int_{\partial\Omega} \frac{\partial u(y, d, k)}{\partial \nu} E(x, y) ds(y), \quad x \in \mathbb{R}^2 \setminus \overline{\Omega}, \tag{2.1}$$

$$u_\infty(\hat{x}, d, k) = -\frac{e^{i\pi/4}}{\sqrt{8\pi k}} \int_{\partial\Omega} \frac{\partial u(y, d, k)}{\partial \nu} e^{-ik\hat{x}\cdot y} ds(y), \tag{2.2}$$

i.e.

$$F(\partial\Omega) = -\eta \int_{\partial\Omega} \frac{\partial u}{\partial \nu}(y) e^{-ik\hat{x}\cdot y} ds(y), \quad \eta := \frac{e^{i\pi/4}}{\sqrt{8\pi k}}.$$

It is also well known [8, 14] that F is Fréchet differentiable. The derivative at $\partial\Omega$ is given by

$$DF(\partial\Omega)q = v_\infty,$$

https://doi.org/10.1017/S0956792515000406 Published online by Cambridge University Press

where q is a vector field in $\mathbb{R}^2$ and v_∞ is the far field pattern of the radiating solution v^s to the Helmholtz equation in $\mathbb{R}^2 \setminus \overline{\Omega}$ satisfying the boundary condition

$$v^s = -q \cdot \nu \frac{\partial u}{\partial \nu} \quad \text{on } \partial\Omega.$$

The integral representation for v_∞ in the backscattering case was introduced in [5]. Similar to (2.1) we have

$$v_\infty(\hat{x}, d, k) = \eta \int_{\partial\Omega} v(y, d, k) \frac{\partial e^{-ik\hat{x}\cdot y}}{\partial \nu} - \frac{\partial v(y, d, k)}{\partial \nu} e^{-ik\hat{x}\cdot y} ds(y).$$

From the substitution $\hat{x} = -d$ and applying the boundary condition (1.1c) and the equation

$$\int_{\partial\Omega} \frac{\partial v(y, d, k)}{\partial \nu} u^s(y, d, k) ds(y) = \int_{\partial\Omega} v(y, d, k) \frac{\partial u^s(y, d, k)}{\partial \nu} ds(y)$$

we deduce that

$$\begin{aligned} v_\infty(-d, d, k) &= \eta \int_{\partial\Omega} v(y, d, k) \frac{\partial u(y, d, k)}{\partial \nu} ds(y) \\ &= -\eta \int_{\partial\Omega} q \cdot \nu \left[\frac{\partial u(y, d, k)}{\partial \nu} \right]^2 ds(y). \end{aligned}$$

Thus,

$$\begin{aligned} D|F_b(\partial\Omega; k)|^2 q &= 2 \operatorname{Re} \overline{F_b(\partial\Omega; k)} D F_b(\partial\Omega; k) q \\ &= \frac{1}{4\pi k} \operatorname{Re} \left[\int_{\partial\Omega} \overline{\frac{\partial u(y, d, k)}{\partial \nu}} e^{-ikd\cdot y} ds(y) \int_{\partial\Omega} q \cdot \nu \left[\frac{\partial u(y, d, k)}{\partial \nu} \right]^2 ds(y) \right]. \end{aligned} \tag{2.3}$$

The main ingredient of our work is high frequency analysis for the obstacle scattering problems justified in [12] and [13]. The Kirchhoff approximation or physical optics approximation, which has commonly been used to simplify the scattering problem in the case of convex scatterers, approximates

$$\frac{\partial u(x, d, k)}{\partial \nu} \approx \begin{cases} 2 \dfrac{\partial u^i(x, d, k)}{\partial \nu} & \text{on } \partial\Omega^- := \{y \in \partial\Omega : \nu(y) \cdot d < 0\} \\ 0 & \text{on } \partial\Omega^+ := \{y \in \partial\Omega : \nu(y) \cdot d \geqslant 0\} \end{cases}$$

for large k. Then the far field pattern for the backscattering follows from (2.2);

$$u_\infty(-d, d, k) \approx -ie^{i\pi/4} \sqrt{\frac{k}{2\pi}} \int_{\partial\Omega^-} e^{2ikd\cdot y} d \cdot \nu(y) ds(y). \tag{2.4}$$

To approximate the integral, we use the method of phase stationary; for smooth functions

https://doi.org/10.1017/S0956792515000406 Published online by Cambridge University Press

ϕ and g in $[a,b]$ such that $\phi' > 0$ in (a,b) and $\phi(t) = \phi(a) + (t-a)^2\phi_1(t), \phi_1(a) \neq 0$,

$$\int_a^b g(t)e^{ik\phi(t)}dt \sim e^{ik\phi(a)} \sum_{n=0}^{\infty} \frac{1}{2(n!)} \Gamma\left(\frac{n+1}{2}\right) h^{(n)}(0) e^{i\pi(n+1)/4} k^{-(n+1)/2} \tag{2.5}$$

$$- e^{ik\phi(b)} \sum_{n=0}^{\infty} \left\{ \frac{1}{\phi'(t)} \frac{d}{dt} \right\}^n \frac{g(t)}{\phi'(t)} \Bigg|_{t=b} (\frac{i}{k})^{n+1} \quad \text{as } k \to \infty, \tag{2.6}$$

where $h^{(n)}(0)$ can be computed from

$$\tau = (\phi(t) - \phi(a))^{1/2}, \quad h(\tau) = g(t)\frac{dt}{d\tau}.$$

Here, the twiddle sign $\sim$ is used for the Poincaré asymptotic expansion, i.e.

$$f(t) \sim \sum_{n=0}^{\infty} a_n t^{-n}, \quad \text{as } t \to \infty$$

means that for every fixed integer $N \geqslant 0$,

$$f(t) = \sum_{n=0}^{N} a_n t^{-n} + O(t^{-N-1}), \quad \text{as } t \to \infty.$$

A proof of the method of phase stationary can be found in many references, for example, see [15]. By considering the first order term,

$$\int_a^b g(t)e^{ik\phi(t)}dt = e^{ik\phi(c)} g(c) \sqrt{\frac{2\pi}{k|\phi''(c)|}} e^{i\pi \mathrm{sgn}(\phi''(c))/4} + O(\frac{1}{k}) \tag{2.7}$$

can be derived. Here, c is assumed to be the only stationary point of ϕ in (a,b).

One may obtain (1.6) by applying the estimation (2.7)–(2.4). The first rigorous way of correcting this heuristic approximation was given by Majda in [12]. As a simple application of (1.6), one can show that a function $F_b(\partial B_R; k)$ converges to $-e^{-2ikR}\sqrt{R/2}$ as $k \to \infty$. More precisely (see the proof of Lemma 1), for sufficiently large k_1

$$\left| F_b(\partial B_R; k) + e^{-2ikR}\sqrt{\frac{R}{2}} \right| \leqslant C \frac{1}{k\sqrt{R}}, \quad kR \geqslant k_1, \tag{2.8}$$

where the constant C is independent of R and k. Then we obtain uniform convergence of

$$G_k(R) := 2|F_b(\partial B_R; k)|^2,$$

since

$$|G_k(R) - R| \leqslant C \frac{1}{k\sqrt{R}} \left(\sqrt{R} + \frac{1}{k\sqrt{R}} \right) \leqslant C \frac{1}{k}.$$

Here, we redefine C accordingly.

https://doi.org/10.1017/S0956792515000406 Published online by Cambridge University Press

Lemma 1 *There is a constant $\tilde{k}_1$ such that if $kR \geqslant \tilde{k}_1$ then*

$$|G_k(R) - R| \leqslant C\frac{1}{k},$$

where C is independent of k and R.

Proof It is enough to show (2.8). Let $u^s(x,d,k)$ be the radiating solution to (1.1) for domain Ω. Let

$$_R\Omega := \{Rx : x \in \Omega\}.$$

Then it is not difficult to show that $w^s(x,d,k/R) := u^s(x/R,d,k)$ solves

$$\begin{aligned}
&\Delta w^s + (\frac{k}{R})^2 w = 0 \text{ in } \mathbb{R}^2 \setminus {}_R\overline{\Omega},\\
&w^s + e^{i(k/R)x\cdot d} = 0 \text{ on } \partial\, {}_R\Omega,\\
&\lim_{r\to\infty} r^{1/2}(\frac{\partial w^s}{\partial r} - i\frac{k}{R}w^s) = 0,\ r = |x|
\end{aligned}$$

and

$$w_\infty(\hat{x},d,k/R) = \sqrt{R}u_\infty(\hat{x},d,k).$$

It follows that

$$F_b(\partial B_R;k/R) = \sqrt{R}F_b(\partial B_1;k).$$

Since (1.6) implies that there is a constant C, which is independent of R and k, such that for $k \geqslant k_1$

$$|F_b(\partial B_1;k) + e^{-2ik}\frac{1}{\sqrt{2}}| \leqslant C\frac{1}{k}.$$

Thus,

$$|F_b(\partial B_R;k/R) + e^{-2i(k/R)R}\sqrt{\frac{R}{2}}| \leqslant C\frac{\sqrt{R}}{k} = C\frac{1}{(k/R)\sqrt{R}}.$$

By redefining k as k/R, we obtain (2.8) as desired. □

Let $\mathbf{Z}_p$ be a class of circles centred at zero with radius $r \geqslant p > 0$. Equivalently, we may consider $\mathbf{Z}_p$ as an interval $[p,\infty)$. Then Lemma 1 implies uniform convergence of $G_k(R)$ to the identity function on $\mathbf{Z}_p$ as $k \to \infty$. However, this does not guarantee the injectivity of $G_k(R)$ nor uniqueness for the inverse problem with circular scatterers. In our approach, we utilise asymptotic analysis for the derivative of F_b. This can be deduced from the method of the stationary phase and the following well-known Theorem stating asymptotic behaviour of the normal derivative $\frac{\partial u}{\partial \nu}$ at the boundary $\partial\Omega$ in [13] (see also [4] for the statement quoted in the following Theorem).

Theorem 2 ([13]) *Let $\Omega \subset \mathbb{R}^2$ be a compact, convex set with smooth boundary $\partial\Omega$ having all principal curvatures everywhere positive. Then the asymptotic behaviour of ψ*

$$\psi := \frac{\partial u}{\partial \nu}e^{-ikx\cdot d}$$

https://doi.org/10.1017/S0956792515000406 Published online by Cambridge University Press

is as follows:

(1) *On the illuminated region* $\partial\Omega^-$

$$\psi(x,k) \sim \sum_{j\geqslant 0} k^{1-j} a_j(x), \tag{2.9}$$

where $a_j(x)$ *are complex-valued* C^∞ *function. More precisely, for any non-negative integers* m, n, *and any multi-index* β

$$|D_x^\beta D_k^n \{\psi(x,k) - \sum_{j=0}^{m} k^{1-j} a_j(x)\}| \leqslant C_{\beta,n,S}(1+k)^{-m-n}$$

on any compact subset S *of* $\partial\Omega^-$.

(2) *In a vicinity of the end points of the shadow boundary* $\partial\Omega^+$, $\psi(x,k)$ *admits the following expansion.*

$$\psi(x,k) \sim \sum_{p,q\geqslant 0} k^{2/3-2p/3-q} b_{p,q}(x) \Psi^{(p)}(k^{1/3} Z(x)), \tag{2.10}$$

where $b_{p,q}$ *and* Ψ *are complex-valued* C^∞ *function and* Z *is a real-valued* C^∞ *function that is positive on* $\partial\Omega^-$, *negative on the interior of* $\partial\Omega^+$, *and vanishes on the end points of* $\partial\Omega^+$. *It satisfies the estimates*

$$\begin{aligned} &|D_x^\beta D_k^n \{\psi(x,k) - \sum_{p,q=0}^{P,Q} k^{2/3-2p/3-q} b_{p,q}(x) \Psi^{(p)}(k^{1/3} Z(x))\}| \\ &\leqslant C_{\beta,n}(1+k)^{-\min\{2P/3,Q\}-2n/3+|\beta|/3} \end{aligned}$$

for any non-negative integers m, P, Q, *and* n.

Moreover, the function Ψ *admits the asymptotic expansion*

$$\Psi(\tau) \sim \sum_{j\geqslant 0} c_j \tau^{1-3j}, \quad \tau \to \infty \tag{2.11}$$

which means that

$$D_\tau^n \{\Psi(\tau) - \sum_{j=0}^{m-1} c_j \tau^{1-3j}\} = O(\tau^{1-3m-n}), \quad \tau \to \infty$$

and Ψ *is rapidly decreasing in the sense of Schwartz as* $\tau \to -\infty$, *i.e. for all non-negative integers* N

$$D_\tau^n \Psi(\tau) = O(\tau^{-N}), \quad \tau \to -\infty.$$

We remark that (2.10) is valid for the entire boundary $\partial\Omega$ by extending $b_{p,q}(x)$ (see [3] and [4]) and that $a_0(x;d) = 2id \cdot \nu(x)$ (i.e. the Kirchhoff approximation). In the following lemma, we compute the next order term $a_1(x;d)$ for the unit circle in the case of backscattering.

https://doi.org/10.1017/S0956792515000406 Published online by Cambridge University Press

Lemma 2 *Suppose that the scatterer is the unit circle. For any $d \in S^1$, the second order term in the asymptotic expansion* (2.9) *at $x = -d$ is given by*

$$a_1(-d;d) = 1.$$

Proof We deduce the following integral equation for $\psi(x,d,k)$ from (2.1) with jump relations (see e.g. [1])

$$\psi(x,d,k) + 2\int_{\partial B_1} \frac{\partial E(x,y)}{\partial \nu(x)} \psi(y,d,k) e^{ikd\cdot(y-x)} ds(y) - 2i \int_{\partial B_1} E(x,y)\psi(y,d,k) e^{ikd\cdot(y-x)} ds(y)$$
$$= 2ikd\cdot \nu(x) - 2i, \quad x \in \partial B_1.$$

Due to Theorem 2, on the illuminated region

$$a_1(x;d) = -2\int_{\partial B_1} \frac{\partial E(x,y)}{\partial \nu(x)} \psi(y,d,k) e^{ikd\cdot(y-x)} ds(y) + O(\frac{1}{k}). \tag{2.12}$$

Here, we apply the boundary condition (1.1c) and (2.1) to remove the second integral.

From the representation of (2.12), $a_1(x;d)$ is determined by the highest order term of the integral, which is dominated by

$$-2\int_{\partial B_1^-} \frac{\partial E(x,y)}{\partial \nu(x)} k a_0(y;d) e^{ikd\cdot(y-x)} ds(y).$$

Since

$$\frac{\partial E(x,y)}{\partial \nu(x)} = -\frac{i}{4} H_1^{(1)}(k|x-y|) k \frac{x-y}{|x-y|}\cdot \nu(x)$$

and $\nu(x) = x$,

$$a_1(-d;d) = \lim_{k\to\infty} -k^2 e^{ik} \int_{\partial B_1^-} H_1^{(1)}(k|d+y|) \frac{(d\cdot y)(1+d\cdot y)}{|d+y|} e^{ikd\cdot y} ds(y).$$

Let

$$d = (-\sin\theta, \cos\theta), \quad y = (\sin(\tau+\theta), -\cos(\tau+\theta))$$

then

$$d\cdot y = -\cos\tau, \quad |d+y| = 2|\sin\frac{\tau}{2}|$$

and thus

$$a_1(-d;d) = \lim_{k\to\infty} 2k^2 e^{ik} \int_0^{\pi/2} H_1^{(1)}\left(2k\sin\frac{\tau}{2}\right) \sin\frac{\tau}{2} \cos\tau e^{-ik\cos\tau} d\tau.$$

Another change of variables $t = 2\sin(\tau/2)$ yields that

$$\cos\frac{\tau}{2} = \frac{\sqrt{4-t^2}}{2}, \quad \cos\tau = 1 - \frac{1}{2}t^2, \quad \frac{d\tau}{dt} = \cos\frac{\tau}{2}$$

https://doi.org/10.1017/S0956792515000406 Published online by Cambridge University Press

and

$$2k^2e^{ik}\int_0^{\pi/2} H_1^{(1)}\left(2k\sin\frac{\tau}{2}\right)\sin\frac{\tau}{2}\cos\tau e^{-ik\cos\tau}d\tau = k^2\int_0^{\sqrt{2}} H_1^{(1)}(kt)\frac{t(2-t)}{\sqrt{4-t^2}}e^{-ikt^2/2}dt.$$

Now, we compute the leading order term of the integral in the right-hand side. Since

$$e^{-ikt^2/2} = \sum_{n=0}^{\infty}\frac{(-ik)^n}{2^n n!}t^{2n},$$

$$\int_0^{\sqrt{2}} H_1^{(1)}(kt)\frac{t(2-t)}{\sqrt{4-t^2}}e^{-ikt^2/2}dt = \sum_{n=0}^{\infty}\frac{(-ik)^n}{2^n n!}\int_0^{\sqrt{2}} H_1^{(1)}(kt)t^{2n+1}\frac{2-t}{\sqrt{4-t^2}}dt.$$

It is known (see pp. 171 of [15]) that

$$\int_0^{\infty} f(t)H_1^{(1)}(kt)dt \sim \frac{1}{\pi}\sum_{s=0}^{\infty} 2^{\alpha_s}e^{i(\alpha_s-1)\pi/2}\Gamma\left(\frac{\alpha_s+2}{2}\right)\Gamma\left(\frac{\alpha_s}{2}\right)\frac{a_s}{k^{\alpha_s+1}}$$

if $f(t)$ has the asymptotic expansion

$$f(t) \sim \sum_{s=0}^{\infty} a_s t^{\alpha_s}, \quad \text{as } t \to 0^+$$

with $\operatorname{Re}(\alpha_0 \pm 1) > -1$ and $\operatorname{Re}\alpha_s \uparrow \infty$ as $s \to \infty$, and there is an $\varepsilon > 0$ such that $f^{(j)}(t) = O(t^{-j-1-s})$ as $t \to \infty$ for $j = 0, 1, 2, \ldots$. Since $t^{2n+1}(2-t)/\sqrt{4-t^2}\chi_{(0,\sqrt{2})}$ satisfies these conditions for each $n = 0, 1, 2, \ldots$, we obtain

$$\int_0^{\sqrt{2}} H_1^{(1)}(kt)t^{2n+1}\frac{2-t}{\sqrt{4-t^2}}dt = O\left(\frac{1}{k^{2n+2}}\right), \quad n = 0, 1, 2, \ldots.$$

Especially,

$$\begin{aligned}\int_0^{\sqrt{2}} H_1^{(1)}(kt)t\frac{2-t}{\sqrt{4-t^2}}dt &= \frac{2}{\pi}\Gamma\left(\frac{3}{2}\right)\Gamma\left(\frac{1}{2}\right)\frac{1}{k^2} + O\left(\frac{1}{k^3}\right)\\ &= \frac{1}{k^2} + O\left(\frac{1}{k^3}\right).\end{aligned}$$

It follows that

$$a_1(-d; d) = 1.$$

□

3 Proof of Theorem 1

We define a map $\mathbf{F}$ on the positive real line such as

$$\mathbf{F} : R \mapsto R - G_k(R) + 2|u_\infty(-d, d, k)|^2 \tag{3.1}$$

https://doi.org/10.1017/S0956792515000406 Published online by Cambridge University Press

for a given far field pattern, $u_\infty(-d,d,k)$, of unknown circular scatterer. Obviously, $2|u_\infty(-d,d,k)|^2$ is a constant. We claim that $\mathbf{F}$ is a contraction mapping on $\mathbf{Z}_{p^2}$ for a sufficiently large k (see Theorem 3), where $p = |u_\infty(-d,d,k)|$. Then $\mathbf{F}$ has a unique fixed point R^* and thus

$$G_k(R^*) = 2|u_\infty(-d,d,k)|^2$$

or (1.4) is uniquely solvable in $\mathbf{Z}_{p^2}$ as stated in Theorem 1.

To this end, we first investigate the asymptotic behaviour of the derivative G_k as follows.

Lemma 3 *Let $\tilde{k} = kR$. Then there is a constant $\tilde{k}_2$ such that if $\tilde{k} \geqslant \tilde{k}_2$ then*

$$|G_k'(R) - 1| < C\frac{1}{\tilde{k}},$$

where C is independent of k and R.

Proof From the definitions of G_k, the derivative G_k' can be understood as Fréchet derivative

$$G_k'(R) = 4\,\mathrm{Re}\,\overline{F_b(\partial B_R;k)}DF_b(\partial B_R;k)v,$$

where v is the outward normal vector at the boundary. It follows from (2.3) and the dilation invariance used in the proof of Lemma 1 that

$$\begin{aligned} G_k'(R) &= \frac{1}{2\pi k}\,\mathrm{Re}\left[\int_{\partial B_R}\overline{\frac{\partial u(y,d,k)}{\partial v}}e^{-ikd\cdot y}ds(y)\int_{\partial B_R}\left[\frac{\partial u(y,d,k)}{\partial v}\right]^2 ds(y)\right] \\ &= \frac{1}{2\pi\tilde{k}}\,\mathrm{Re}\left[\int_{\partial B_1}\overline{\frac{\partial u(y,d,\tilde{k})}{\partial v}}e^{-i\tilde{k}d\cdot y}ds(y)\int_{\partial B_1}\left[\frac{\partial u(y,d,\tilde{k})}{\partial v}\right]^2 ds(y)\right]. \end{aligned}$$

Here, by u in the second line we mean the solution to (1.1) with the unit circle scatterer to avoid too much notation.

To estimate these integrals, we use the result from [13], Theorem 2, and the method of stationary phase. First, we split the domain into the illuminated region, ∂B_1^-, and shadow region, ∂B_1^+ according to

$$\int_{\partial B_1}\frac{\partial u(y,d,\tilde{k})}{\partial v}e^{i\tilde{k}d\cdot y}ds(y) = \int_{\partial B_1^-}\frac{\partial u(y,d,\tilde{k})}{\partial v}e^{i\tilde{k}d\cdot y}ds(y) + \int_{\partial B_1^+}\frac{\partial u(y,d,\tilde{k})}{\partial v}e^{i\tilde{k}d\cdot y}ds(y), \tag{3.2}$$

$$\int_{\partial B_1}\left[\frac{\partial u(y,d,\tilde{k})}{\partial v}\right]^2 ds(y) = \int_{\partial B_1^-}\left[\frac{\partial u(y,d,\tilde{k})}{\partial v}\right]^2 ds(y) + \int_{\partial B_1^+}\left[\frac{\partial u(y,d,\tilde{k})}{\partial v}\right]^2 ds(y). \tag{3.3}$$

Let

$$d = (-\sin\theta, \cos\theta), \quad y = (\sin\tau, -\cos\tau)$$

and

$$\phi := 2d(\theta)\cdot y(\tau) = -2\cos(\tau-\theta), \quad \psi := \frac{\partial u}{\partial v}e^{-ikd\cdot y}.$$

https://doi.org/10.1017/S0956792515000406 Published online by Cambridge University Press

Then,

$$\int_{\partial B_1^-} \frac{\partial u(y,d,\tilde{k})}{\partial \nu} e^{i\tilde{k}d\cdot y} ds(y) = \int_{-\pi/2+\theta}^{\pi/2+\theta} \psi(y(\tau),d(\theta),\tilde{k}) e^{i\tilde{k}\phi(\tau)} d\tau, \tag{3.4}$$

$$\int_{\partial B_1^+} \frac{\partial u(y,d,\tilde{k})}{\partial \nu} e^{i\tilde{k}d\cdot y} ds(y) = \int_{\pi/2+\theta}^{3\pi/2+\theta} \psi(y(\tau),d(\theta),\tilde{k}) e^{i\tilde{k}\phi(\tau)} d\tau, \tag{3.5}$$

$$\int_{\partial B_1^-} \left[\frac{\partial u(y,d,\tilde{k})}{\partial \nu}\right]^2 ds(y) = \int_{-\pi/2+\theta}^{\pi/2+\theta} \psi^2(y(\tau),d(\theta),\tilde{k}) e^{i\tilde{k}\phi(\tau)} d\tau, \tag{3.6}$$

$$\int_{\partial B_1^+} \left[\frac{\partial u(y,d,\tilde{k})}{\partial \nu}\right]^2 ds(y) = \int_{\pi/2+\theta}^{3\pi/2+\theta} \psi^2(y(\tau),d(\theta),\tilde{k}) e^{i\tilde{k}\phi(\tau)} d\tau. \tag{3.7}$$

Note that for a fixed $d(\theta)$, the illuminated and shaded regions are as follows:

$$\partial B_1^- := \{y \in \partial B_1 : \nu(y)\cdot d(\theta) < 0\} = \{\tau : -\frac{\pi}{2} + \theta < \tau < \frac{\pi}{2} + \theta\},$$
$$\partial B_1^+ := \{y \in \partial B_1 : \nu(y)\cdot d(\theta) \geqslant 0\} = \{\tau : \frac{\pi}{2} + \theta \leqslant \tau \leqslant \frac{3\pi}{2} + \theta\}.$$

Also, the phase function $\phi(\tau)$ has only one stationary point at

$$\tau = \theta, \quad \tau = \theta + \pi$$

on ∂B_1^- and ∂B_1^+, respectively.

We consider integral (3.5) first. Since on a neighbourhood of ∂B_1^+

$$\psi(y,d,\tilde{k}) \sim \sum_{p,q\geqslant 0} \tilde{k}^{2/3-2p/3-q} b_{p,q}(y) \Psi^{(p)}(\tilde{k}^{1/3} Z(y)), \quad b_{0,0} = \frac{\nu\cdot d}{Z} \tag{3.8}$$

the leading order term of integral (3.5) is

$$-\int_{\pi/2+\theta}^{3\pi/2+\theta} \tilde{k}^{2/3} \frac{\cos(\tau-\theta)}{Z(y(\tau))} \Psi(\tilde{k}^{1/3} Z(y(\tau))) e^{i\tilde{k}\phi(\tau)} d\tau.$$

Now, we apply the method of phase stationary. Due to the asymptotic behaviour of ψ in the deep shadow region, especially at the only stationary point of ϕ, the integral is governed by the boundary value of the integrand. However, the boundary terms would be cancelled out with the boundary terms of the principle term of ψ in (3.4), because the representation (3.8) or (2.10) is valid for entire ∂B_1 as mentioned below Theorem 2. This holds for all other orders of ψ near the boundary of ∂B_1^+. Consequently, the leading order term of (3.2) is determined by asymptotic expansion (2.9)

$$\psi(y,d,\tilde{k}) = \tilde{k} a_0(y;d) + a_1(y;d) + O(\frac{1}{\tilde{k}})$$

over the illuminated region. More precisely, the leading order term of (3.2) is given by

$$\int_{-\pi/2+\theta}^{\pi/2+\theta} \psi(y(\tau),d,\tilde{k}) e^{i\tilde{k}\phi(\tau)} d\tau = \tilde{k}\left(b_{01}\frac{1}{\sqrt{\tilde{k}}} + b_{02}\frac{1}{\tilde{k}\sqrt{\tilde{k}}}\right) + b_{11}\frac{1}{\sqrt{\tilde{k}}} + O\left(\frac{1}{\tilde{k}\sqrt{\tilde{k}}}\right),$$

https://doi.org/10.1017/S0956792515000406 Published online by Cambridge University Press

where

$$\int_{-\pi/2+\theta}^{\pi/2+\theta} a_0(y(\tau);d(\theta))e^{i\tilde{k}\phi(\tau)}d\tau = b_{01}\frac{1}{\sqrt{\tilde{k}}} + b_{02}\frac{1}{k\sqrt{\tilde{k}}} + O\left(\frac{1}{\tilde{k}^2}\right), \tag{3.9}$$

$$\int_{-\pi/2+\theta}^{\pi/2+\theta} a_1(y(\tau);d(\theta))e^{i\tilde{k}\phi(\tau)}d\tau = b_{11}\frac{1}{\sqrt{\tilde{k}}} + O\left(\frac{1}{\tilde{k}}\right). \tag{3.10}$$

We note that the leading order terms appearing in (3.9) and (3.10) are computed from the stationary point of ϕ rather than the boundary terms of a_0 and a_1.

Similarly, a few leading order terms of the integral (3.3) can be computed as follows:

$$\begin{aligned}
&\int_{-\pi/2+\theta}^{\pi/2+\theta} \psi^2(y(\tau),d,\tilde{k})e^{i\tilde{k}\phi(\tau)}d\tau \\
&\quad= \tilde{k}^2\int_{-\pi/2+\theta}^{\pi/2+\theta} a_0^2(y(\tau);d(\theta))e^{i\tilde{k}\phi(\tau)}d\tau + 2\tilde{k}\int_{-\pi/2+\theta}^{\pi/2+\theta} a_0(y(\tau);d(\theta))a_1(y(\tau);d(\theta))e^{i\tilde{k}\phi(\tau)}d\tau \\
&\qquad+ O\left(\frac{1}{\sqrt{\tilde{k}}}\right) \\
&\quad= \tilde{k}^2\left(c_{01}\frac{1}{\sqrt{\tilde{k}}} + c_{02}\frac{1}{\tilde{k}\sqrt{\tilde{k}}}\right) + 2\tilde{k}c_{11}\frac{1}{\sqrt{\tilde{k}}} + O\left(\frac{1}{\sqrt{\tilde{k}}}\right),
\end{aligned}$$

where

$$\int_{-\pi/2+\theta}^{\pi/2+\theta} a_0^2(y(\tau);d(\theta))e^{i\tilde{k}\phi(\tau)}d\tau = c_{01}\frac{1}{\sqrt{\tilde{k}}} + c_{02}\frac{1}{\tilde{k}\sqrt{\tilde{k}}} + O\left(\frac{1}{\tilde{k}^2}\right), \tag{3.11}$$

$$\int_{-\pi/2+\theta}^{\pi/2+\theta} a_0(y(\tau);d(\theta))a_1(y(\tau);d(\theta))e^{i\tilde{k}\phi(\tau)}d\tau = c_{11}\frac{1}{\sqrt{\tilde{k}}} + O\left(\frac{1}{\tilde{k}}\right). \tag{3.12}$$

From a method similar to that used in the proof of Lemma 1 together with the stationary phase method, one has that

$$\begin{aligned}
b_{01}\frac{1}{\sqrt{\tilde{k}}} + b_{02}\frac{1}{\tilde{k}\sqrt{\tilde{k}}} &= e^{-2i\tilde{k}+i\pi/4}\sqrt{\pi}\Big[-2i\frac{1}{\sqrt{\tilde{k}}} - \frac{3}{8}\frac{1}{\tilde{k}\sqrt{\tilde{k}}}\Big], \\
b_{11}\frac{1}{\sqrt{\tilde{k}}} &= e^{-2i\tilde{k}+i\pi/4}\sqrt{\pi}\frac{1}{\sqrt{\tilde{k}}}, \\
c_{01}\frac{1}{\sqrt{\tilde{k}}} + c_{02}\frac{1}{\tilde{k}\sqrt{\tilde{k}}} &= e^{-2i\tilde{k}+i\pi/4}\sqrt{\pi}\Big[-4\frac{1}{\sqrt{\tilde{k}}} + \frac{7}{4}i\frac{1}{\tilde{k}\sqrt{\tilde{k}}}\Big], \\
c_{11} &= b_{11}.
\end{aligned}$$

We refer the reader to Appendix for detailed computation for b_{lm} and c_{lm}.

Finally, we have the following asymptotic form:

$$\begin{aligned}
G_k'(\zeta) &= \frac{1}{2\pi}\,\mathrm{Re}\left[\overline{c_{01}}d_{01}\tilde{k} + (\overline{c_{02}+c_{11}})d_{01} + (d_{02}+2d_{11})\overline{c_{01}}\right] + O\left(\frac{1}{\tilde{k}}\right) \\
&= 1 + O\left(\frac{1}{\tilde{k}}\right)
\end{aligned}$$

as desired. □

https://doi.org/10.1017/S0956792515000406 Published online by Cambridge University Press

Theorem 3 *For a given $p > 0$, there exists $k_0 > 0$ such that if $k \geqslant k_0$ then $\mathbf{F}$ is a contraction mapping from $\mathbf{Z}_{p^2}$ to itself.*

Proof For given $p > 0$, let

$$k_1 = \max\left\{\frac{C}{p^2}, \frac{\tilde{k}_1}{p^2}\right\},$$

where $\tilde{k}_1$ and C appear in Lemma 1. Then Lemma 1 implies that

$$\mathbf{F}(R) = R - G_k(R) + 2p^2 \geqslant p^2, \quad R \in \mathbf{Z}_{p^2}$$

as long as $k \geqslant k_1$. Thus, $\mathbf{F}$ is a function from $\mathbf{Z}_{p^2}$ to itself. In order to show it is a contraction mapping, we take $\tilde{k}_2$ in Lemma 3 so that

$$|G_k'(R) - 1| < \frac{1}{2}, \quad kR \geqslant \tilde{k}_2. \tag{3.13}$$

Let

$$k_0 = \max\left\{k_1, \frac{\tilde{k}_2}{p^2}\right\}.$$

Then for any $R_1, R_2 \in \mathbf{Z}_{p^2}$

$$\begin{aligned} |\mathbf{F}(R_2) - \mathbf{F}(R_1)| &= |(R_2 - R_1) - (G_k(R_2) - G_k(R_1))| \\ &\leqslant |1 - G_k'(R_0)||R_2 - R_1| \end{aligned}$$

for some $R_0 \in \mathbf{Z}_{p^2}$. It follows that

$$|\mathbf{F}(R_2) - \mathbf{F}(R_1)| < \frac{1}{2}|R_2 - R_1|$$

as long as $k \geqslant k_0$. □

We remark that it might be possible to obtain (3.13) from the series representation of far field pattern and properties of the Bessel and Neumann functions. With this approach, one may have estimates of $k_0 p^2$ and extend the uniqueness result to three dimensions.

4 Frozen Newton method

In this section, we introduce an iteration method to solve the inverse obstacle scattering problem with modulus data for a convex domain.

We begin with normalising scatterers. As mentioned in Section 1, the modulus data cannot determine the location of a scatterer. Thus, it is important to normalise scatterers. To this end, we translate scatterers so that they are located above the x-axis and the origin is the tangential point of $\partial\Omega$. Since we assume that the scatterers in our problem are strictly convex, the boundary curve $\partial\Omega$ can be uniquely represented by the parameter θ, the angle from the positive x_1-axis to the tangent line at $y(\theta)$ in counterclockwise orientation as shown in Figure 1. From this parameter θ, the unit tangent and outward

https://doi.org/10.1017/S0956792515000406 Published online by Cambridge University Press

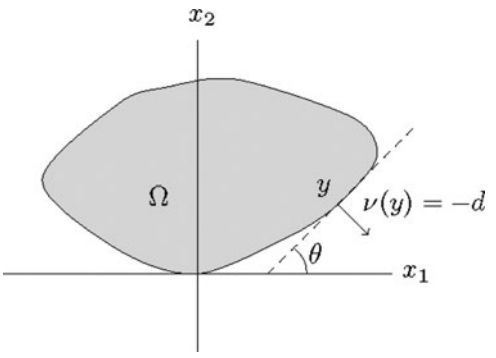


FIGURE 1. Normalised scatterer.

normal vectors at $y(\theta)$ are given by

$$T(\theta) = (\cos\theta, \sin\theta),$$
$$\nu(\theta) = (\sin\theta, -\cos\theta).$$

Since the derivative of T with respect to the arc length s, $dT/ds = -\kappa\nu$ for the curvature κ,

$$\frac{dT}{d\theta}\frac{d\theta}{ds} = -\kappa\nu$$

or

$$\frac{ds}{d\theta} = \frac{1}{\kappa} =: \zeta.$$

On the other hand,

$$\frac{dy}{ds} = \frac{dy}{d\theta}\frac{d\theta}{ds} = T.$$

Thus, we obtain a unique representation of a normalised convex scatterer,

$$y(\theta) = \int_0^\theta \zeta(\tau)(\cos\tau, \sin\tau)d\tau. \tag{4.1}$$

Now, we define a map Φ from a subset $\mathbf{Z}$ of a set of smooth 2π-periodic functions to a class $\mathbf{S}$ of normalised strictly convex scatterers by (4.1),

$$\Phi : \mathbf{Z} \to \mathbf{S},$$
$$\zeta \mapsto \partial\Omega.$$

We remark that

$$\mathbf{Z} \perp \{\sin\theta, \cos\theta\} \tag{4.2}$$

in L^2 sense because $y(0) = y(2\pi)$.

Let the direction d for the incident field $u^i = e^{ikd\cdot x}$ be

$$d(\theta) = -(\sin\theta, -\cos\theta).$$

https://doi.org/10.1017/S0956792515000406 Published online by Cambridge University Press

Similar to the circle case, we define a map G_k with this notation;

$$G_k : \zeta(\theta) \mapsto 2|u_\infty(-d(\theta), d(\theta), k)|^2$$

or equivalently

$$G_k(\zeta) = 2|F_b(\Phi(\zeta); k)|^2.$$

Then, the inverse obstacle scattering problem with modulus data, (1.4) is to seek ζ for given $|u_\infty(-d(\theta), d(\theta), k)|$ satisfying

$$G_k(\zeta) = 2|u_\infty(-d, d, k)|^2. \tag{4.3}$$

Several numerical schemes to solve the non-linear equation (4.3) involve iteration methods generated by

$$\zeta_{n+1} = \zeta_n - A_n[G_k(\zeta_n) - 2|u_\infty(-d, d, k)|^2] \tag{4.4}$$

for some operator A_n. One of the common methods is Newton's method which $A_n = [DG_k(\zeta_n)]^{-1}$ leads to. However, Newton's method requires invertibility of the linearised map at each step, which is unknown, as well as high computational cost. To avoid these difficulties, we fix A_n as the high-frequency limit of $[DG_k(\zeta_n)]^{-1}$. To this end, we rewrite (1.6) in terms of our parameter θ as follows:

$$|u_\infty(-d(\theta), d(\theta), k) + e^{2iky(\theta)\cdot d(\theta)}\sqrt{\frac{\zeta(\theta)}{2}}| \leqslant C\frac{1}{k}, \quad k \geqslant k_0.$$

Thus,

$$\lim_{k\to\infty} G_k(\zeta) = \zeta.$$

Although it shows that G_k converges to the identity map only pointwisely, from the result in the previous section one may expect that

$$\lim_{k\to\infty} DG_k = I$$

in some sense. For this reason, we set

$$A_n = I.$$

It follows that

$$\zeta_{n+1} = \zeta_n - G_k(\zeta_n) + 2|u_\infty(-d, d, k)|^2.$$

This iteration scheme is equivalent to seeking a fixed point of a map

$$\mathbf{F} : \zeta \mapsto \zeta - G_k(\zeta) + 2|u_\infty(-d, d, k)|^2 \tag{4.5}$$

in the class $\mathbf{Z}$. We notice that (3.1) is a restricted map of (4.5) to circular domains.

Although we believe that

$$G_k(\mathbf{Z}) \perp \{\sin\theta, \cos\theta\} \tag{4.6}$$

https://doi.org/10.1017/S0956792515000406 Published online by Cambridge University Press

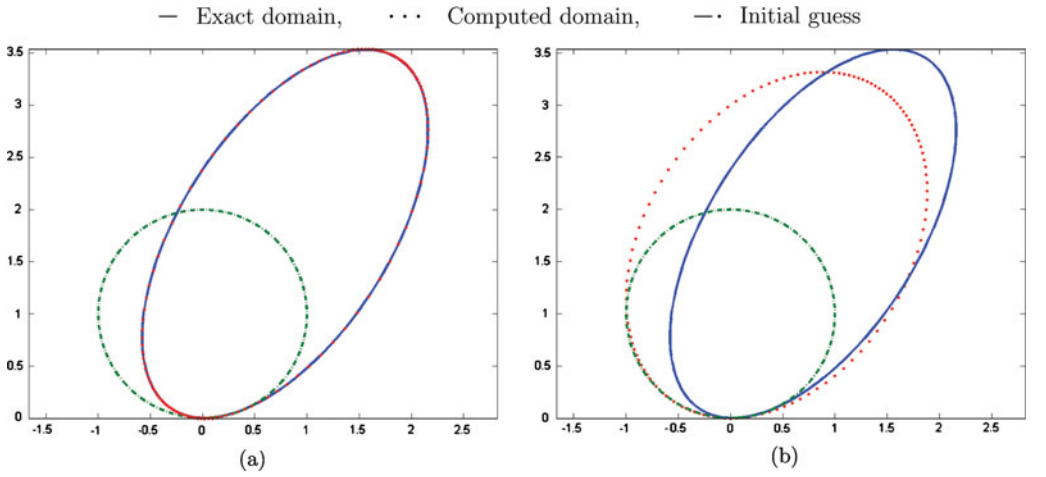


FIGURE 2. Reconstructed scatterer, ellipse. (a) $k = 2.5$, $kR \approx 5$, after 10 iterations. (b) $k = 0.1$, $kR \approx 0.2$, after 50 iterations.

from numerical evidence, we could not prove it analytically at this point. For this reason, we apply a projection operator P

$$P : L^2(S^1) \to \{\sin\theta, \cos\theta\}^{\perp}$$

to the mapping $\mathbf{F}$. Thus, one may use the iteration scheme

$$\zeta_{n+1} = \zeta_n - P(G_k(\zeta_n) - 2|u_\infty(-d, d, k)|^2). \tag{4.7}$$

In particular, applying the projection operator may be understood as a regularisation method in the case of noise data.

We remark that to show (4.6), which characterises far field patterns for convex domains, is an interesting problem itself. Indeed, it is a general result of Kress and Rundell's work ([9]);

$$D|F(\partial B_1)|^2 q = 0, \quad q = \cos\theta, \sin\theta.$$

Figure 2 shows a reconstructed scatterer from the method (4.7) with different k values. To solve the direct problem, we follow the numerical method described in [1]. A more non-trivial example is given in Figure 3 with noisy data.

5 Conclusion

In this work, we provided an iterative numerical algorithm to reconstruct convex scatterers from phaseless backscattering data. In this algorithm, we do not need the Fréchet derivative of F_b or $|F_b|$ so we avoid the additional cost of computing the derivative DF_b. Furthermore, one may have a stability result by showing convergence since the algorithm is based on a fixed point argument.

https://doi.org/10.1017/S0956792515000406 Published online by Cambridge University Press

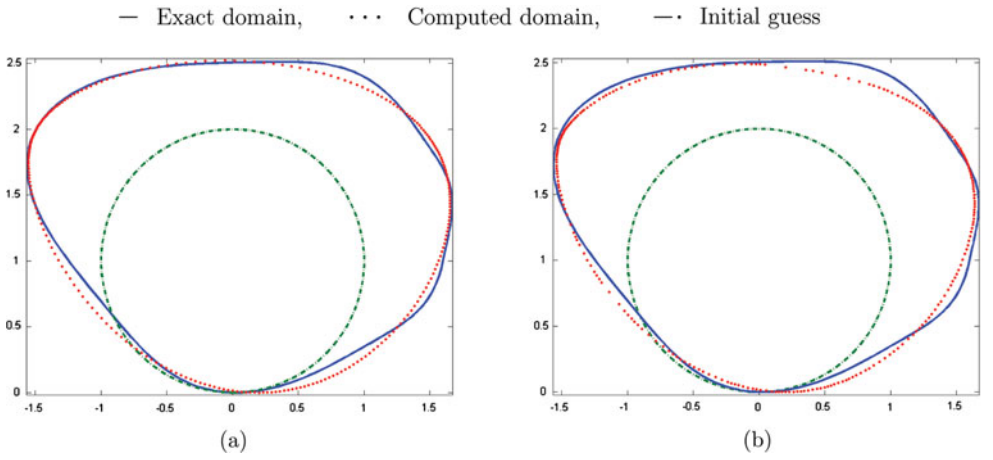


FIGURE 3. Reconstructed scatterer, $r(\theta) = 1/(1 + 0.6\cos\theta - 0.04\sin 5\theta)$. (a) $k = 0.5$, $kR \approx 1$, after 50 iterations. (b) $k = 0.5$, $kR \approx 1$, 3% noise level, after 50 iterations.

From the theoretical point of view, this iteration method is a tool for uniqueness results of the inverse problems. In particular, we showed certain existence and uniqueness for the inverse problem assuming scatterers are circles.

The next step of our work is to analyse the proposed numerical method for more general convex domains. This includes certain convergence results of the iteration scheme and effects of the general ill-posedness of the inverse obstacle problem to the numerical solutions. This requires computation of $a_1(y;d)$ for convex domains and characterisation of the far field patterns such as (4.6).

References

[1] COLTON, D. & KRESS, R. (1998) *Inverse Acoustic and Electromagnetic Scattering Theory*, 2nd ed., Applied Mathematical Sciences, Vol. 93, Springer-Verlag, Berlin.

[2] COLTON, D. & SLEEMAN, B. D. (1983) Uniqueness theorems for the inverse problem of acoustic scattering. *IMA J. Appl. Math.* **31**(3), 253–259.

[3] DOMÍNGUEZ, V., GRAHAM, I. G. & SMYSHLYAEV, V. P. (2007) A hybrid numerical-asymptotic boundary integral method for high-frequency acoustic scattering. *Numer. Math.* **106**(3), 471–510.

[4] ECEVIT, F. & REITICH, F. (2009) Analysis of multiple scattering iterations for high-frequency scattering problems. I: The two-dimensional case. *Numer. Math.* **114**(2), 271–354.

[5] HÄHNER, P. & KRESS, R. (2000) Uniqueness for a linearized, inverse obstacle problem using backscattering data. In: *Proceedings of the Fifth International Conference on Mathematical and Numerical Aspects of Wave Propagation (Santiago de Compostela, 2000)*, SIAM, Philadelphia, PA, pp. 488–493.

[6] IVANYSHYN, O. (2007) Shape reconstruction of acoustic obstacles from the modulus of the far field pattern. *Inverse Probl. Imaging.* **1**(4), 609–622.

[7] IVANYSHYN, O. & KRESS, R. (2010) Identification of sound-soft 3D obstacles from phaseless data. *Inverse Probl. Imaging.* **4**(1), 131–149.

[8] KIRSCH, A. (1993) The domain derivative and two applications in inverse scattering theory. *Inverse Problems.* **9**(1), 81–96.

https://doi.org/10.1017/S0956792515000406 Published online by Cambridge University Press

[9] Kress, R. & Rundell, W. (1997) Inverse obstacle scattering with modulus of the far field pattern as data. In: *Inverse Problems in Medical Imaging and Nondestructive Testing (Oberwolfach, 1996)*, Springer, Vienna, pp. 75–92.
[10] Kress, R. & Rundell, W. (1999) Inverse obstacle scattering using reduced data. *SIAM J. Appl. Math.* **59**(2), 442–454 (electronic).
[11] Liu, X. & Zhang, B. (2010) Unique determination of a sound-soft ball by the modulus of a single far field datum. *J. Math. Anal. Appl.* **365**(2), 619–624.
[12] Majda, A. (1976) High frequency asymptotics for the scattering matrix and the inverse problem of acoustical scattering. *Comm. Pure Appl. Math.* **29**(3), 261–291.
[13] Melrose, R. B. & Taylor, M. E. (1985) Near peak scattering and the corrected Kirchhoff approximation for a convex obstacle. *Adv. Math.* **55**(3), 242–315.
[14] Potthast, R. (1994) Fréchet differentiability of boundary integral operators in inverse acoustic scattering. *Inverse Problems.* **10**(2), 431–447.
[15] Wong, R. (1989) *Asymptotic Approximations of Integrals*, Computer Science and Scientific Computing. Academic Press Inc., Boston, MA.

Appendix A

Here, we compute the coefficients b_{lm} and c_{lm} in (3.9)–(3.12).

We rewrite the left-hand side of (3.9) using $a_0(y,d) = 2id \cdot v(y)$ and $t = \tau - \theta$;

$$\int_{-\pi/2+\theta}^{\pi/2+\theta} a_0(y(\tau); d(\theta)) e^{i\tilde{k}\phi(\tau)} d\tau = -4i \int_0^{\pi/2} \cos t e^{-2i\tilde{k}\cos t} dt.$$

Here, we use

$$\phi(\tau) = -2\cos(\tau - \theta), \quad d(\theta) \cdot v(y(\tau)) = -\cos(\tau - \theta).$$

Since 0 is the only stationary point for $\cos t$ over $[0, \pi/2]$, it follows from the stationary phase method that

$$\begin{aligned}\int_0^{\pi/2} &\cos t e^{-2i\tilde{k}\cos t} dt \\ &= e^{-2i\tilde{k}} \left[\frac{1}{2} \Gamma\left(\frac{1}{2}\right) h(0) e^{i\pi/4} \tilde{k}^{-1/2} + \frac{1}{2} \Gamma(1) h^{(1)}(0) e^{i\pi/2} \tilde{k}^{-1} + \frac{1}{4} \Gamma\left(\frac{3}{2}\right) h^{(2)}(0) e^{i3\pi/4} \tilde{k}^{-3/2} \right] \\ &\quad + \mathcal{O}\left(\frac{1}{\tilde{k}^2}\right).\end{aligned}$$

Here, $h(\tau)$ is defined as

$$h(\tau) = g(t)\frac{dt}{d\tau}, \quad g(t) = -\cos t, \quad \tau = 2\sin\frac{t}{2}.$$

Note that, the first order boundary term (2.6) vanishes.

We deduce that

$$h(\tau) = \frac{\tau^2 - 2}{\sqrt{4 - \tau^2}} \tag{A 1}$$

and

$$h^{(1)}(\tau) = \frac{-\tau^3 + 6\tau}{(4-\tau^2)^{3/2}}, \quad h^{(2)}(\tau) = \frac{24}{(4-\tau^2)^{5/2}}.$$

https://doi.org/10.1017/S0956792515000406 Published online by Cambridge University Press

Thus, we obtain

$$b_{01}\frac{1}{\sqrt{\tilde{k}}}+b_{02}\frac{1}{k\sqrt{\tilde{k}}}=e^{-2i\tilde{k}+i\pi/4}\sqrt{\pi}\Big[-2i\frac{1}{\sqrt{\tilde{k}}}-\frac{3}{8}\frac{1}{\tilde{k}\sqrt{\tilde{k}}}\Big].$$

In (3.10), the corresponding $h(\tau)=2/\sqrt{4-\tau^2}$. Thus,

$$h(0)=1$$

and

$$b_{11}\frac{1}{\sqrt{\tilde{k}}}=e^{-2i\tilde{k}+i\pi/4}\sqrt{\pi}\frac{1}{\sqrt{\tilde{k}}}.$$

As for (3.11), since $g(t)=-4\cos^2 t$

$$h(\tau)=-2\frac{(2-\tau^2)^2}{\sqrt{4-\tau^2}}$$

and

$$h^{(1)}(\tau)=2\frac{\tau(3\tau^4-20\tau^2+28)}{(4-\tau^2)^{3/2}},$$
$$h^{(2)}(\tau)=-\frac{12\tau^6-120\tau^4+368\tau^2-224}{(4-\tau^2)^{5/2}}.$$

Thus,

$$h(0)=-4,\quad h^{(1)}(0)=0,\quad h^{(2)}(0)=7$$

and

$$c_{01}\frac{1}{\sqrt{\tilde{k}}}+c_{02}\frac{1}{\tilde{k}\sqrt{\tilde{k}}}=e^{-2i\tilde{k}+i\pi/4}\sqrt{\pi}\Big[-4\frac{1}{\sqrt{\tilde{k}}}+\frac{7}{4}i\frac{1}{\tilde{k}\sqrt{\tilde{k}}}\Big].$$

Since $a_1(-d;d)=1$ from Lemma 2 and the phase function ϕ has the stationary point at $y=-d$, $h(0)$ corresponding to (3.12) is the same as the value of $h(\tau)$ in (A 1) at $\tau=0$. As a consequence,

$$c_{11}=b_{01}.$$

https://doi.org/10.1017/S0956792515000406 Published online by Cambridge University Press